Towards Integrated Target–SOL–Core Plasma Simulations for Fusion Devices with Liquid Metal Targets

Journal of Fusion Energy (2023)42:41
https://doi.org/10.1007/s10894-023-00377-5

RESEARCH

Towards Integrated Target–SOL–Core Plasma Simulations for Fusion Devices with Liquid Metal Targets

Giuseppe Francesco Nallo[1] · Jorge Gonzalez[2] · Elisabetta Bray[1] · Teobaldo Luda di Cortemiglia[3] · Chiara Marchetto[4] · Fabio Subba[1] · Egbert Westerhof[2] · Roberto Zanino[1]

Accepted: 2 August 2023

Abstract
Self-healing liquid metal divertors (LMDs) based on the Capillary Porous Structure (CPS) concept are currently being considered among the possible solutions to the power exhaust problem in future fusion reactors. Indeed, the passive replenishment of the plasma-facing surface by capillary forces and the self-shielding of the target via vapor emission can potentially improve the divertor lifetime and its resilience to transient loads. On the other hand, the LMD target erosion can be significant due to evaporation and thermal sputtering, on top of physical sputtering, possibly leading to unacceptable core plasma dilution/power losses (for a low-*Z*/high-*Z* metal such as Li and Sn, respectively). For this reason, it is necessary to assess whether an LMD is compatible with an European DEMO (EU-DEMO) plasma scenario. This requires a self-consistent model of the impurity emission from the target, the plasma in both the scrape-off layer (SOL) and the core regions and the transport of impurities therein. In this paper, an an integrated modelling approach is proposed, which is based on SOLPS-ITER and includes its coupling with a target erosion model written in FreeFem++ and a core plasma model (ASTRA/STRAHL). An application of the coupled SOL-target model to simulate experiments performed in the Magnum-PSI linear plasma device with a CPS target filled with Li is also included to provide a first demonstration of the capabilities of the approach. Results are promising, being in good agreement (within a few degrees) with the measured target temperature distribution. In perspective, the modelling framework presented here will be applied to the EU-DEMO with an Sn divertor.

Keywords Liquid metal divertors · Integrated modelling · SOLPS-ITER · ASTRA · STRAHL

Introduction

The development of a reliable solution to the power exhaust problem in nuclear fusion reactors is among the milestones listed in the European Research Roadmap to the Realisation of Fusion Energy [1]. The baseline strategy, which was conceived for ITER, consists in using actively cooled tungsten (W) monoblocks as divertor plates, resorting to impurity (e.g., Ne, Ar or Xe) seeding to achieve at least partially detached plasma operation [2]. For European DEMO (EU-DEMO)-sized reactors, however, tolerable target heat fluxes can only be attained through radiation of a percentage of the power crossing the separatrix larger than 90%. This results in an operating condition the stability of which is still to be proven [3, 4]. Moreover, the larger amount of energy stored in the plasma will require ELMs to be either avoided or strongly mitigated. The effects of neutron irradiation will also represent an unprecedented challenge for both structural and plasma-facing materials [4]. Therefore, alternative strategies are being investigated within EUROfusion, including advanced magnetic configurations [5] and self-healing Liquid Metal Divertors (LMDs) based on the Capillary Porous Structure (CPS) concept [6, 7], for which the most promising Liquid Metals (LMs) are Li, Sn and Li–Sn [8].

For a CPS-based LMD, the erosion of the plasma-facing surface is compensated by the continuous and passive replenishment with fresh LM provided by capillary forces. Moreover, the vapor shielding phenomenon, which is intrinsically self-regulating, can increase the component resilience to transient events, including ELMs [9]. LM-filled CPS targets were successfully exposed to tokamak

Extended author information available on the last page of the article

Published online: 23 August 2023

conditions both in limiter and in divertor configuration (for instance in FTU and COMPASS, respectively) [10–12]. Experiments in Linear Plasma Devices (LPDs) also allowed to characterize the interactions between plasma and LM targets in a more controlled and thoroughly diagnosed environment [13].

Among the challenges associated to the use of LMs as plasma-facing components there are evaporation and sputtering, which might lead to unacceptable core plasma dilution/power losses (for Li/Sn, respectively) [14]. The compliance of a proposed LMD design with an EU-DEMO-relevant plasma scenario should thus be assessed in terms of:

- The peak heat flux to the CPS-coated target, which must not overcome the power handling limit of the component itself;
- The core plasma contamination/dilution, which must be compatible with the desired fusion performance.

To contribute to this assessment through modelling, it is necessary to simulate the Scrape-Off Layer (SOL) plasma transport, the erosion of impurities from the target and their transport in the SOL and core, including their interactions with the plasma. These physical processes are mutually interacting, thereby requiring self-consistent models to be employed.

Integrated target-SOL-core calculations were carried out in the past by means of the COREDIV code to explore the possible operational space of an EU-DEMO with an LMD [15]. More recently, similar calculations were carried out for the DTT device [16]. COREDIV is a comprehensive tool which provides self-consistent results in a short time, but also adopts a number of simplifications, including a fluid treatment of the neutral species, a 1D thermal model of the target, a slab model for the SOL and an *a priori* neglected impurity pinch in the core.

In the attempt of providing more quantitative evaluations, one possibility is to adopt specialized tools for the target, SOL and core modelling, respectively, coupling them together. This paper aims at presenting two main recent advances in this line of activity:

- The self-consistent coupling between a LM target erosion model and a SOL plasma model based on SOLPS-ITER, a state-of-the-art code for the SOL plasma and neutrals transport in tokamaks;
- The one-way coupling between SOLPS-ITER and STRAHL, a code for the impurity transport in the core plasma, running within the ASTRA modelling framework.

As far as the target-SOL coupling is concerned, this paper also provides first results from the application of SOLPS-ITER coupled to a target model to Magnum-PSI experiments. The SOL-core coupling is instead the subject of ongoing work, therefore results shall be presented in a future work.

The paper is organized as follows. In Sect. 2, after an overview of the proposed modelling approach, the tools adopted for the target, SOL and core plasma, respectively, are described, together with the coupling algorithm. Section 3 then reports first applications of subsets of the integrated model to Magnum-PSI. Section 4 describes ongoing work regarding the SOL-core model. Finally, Sect. 5 describes future plans for this activity.

Methodology

Overview of the Modelling Approach

In this work, the following models were adopted:

- A 2D SOL plasma model (B2.5 in SOLPS-ITER) to compute SOL plasma temperature and density distributions while self-consistently computing the radiated power in the SOL and the heat flux on the divertor targets;
- A 2D neutral model (Eirene in SOLPS-ITER) to compute neutrals temperature and density distributions, accounting for their interactions with the plasma and for pumping/redeposition;
- A 2D LM erosion model (developed in FreeFem++ [17]) to compute target temperature distribution and LM evaporation/sputtering rates;
- A 1.5D core plasma model (ASTRA+TGLF+−STRAHL) to compute core plasma temperature and density profiles, and radiated power in core.

In the following, a brief description of each model is provided.

SOL Plasma and Neutrals Model: SOLPS-ITER

SOLPS-ITER is composed of a 2D multi-fluid plasma solver (B2.5) and of a 2D kinetic neutral model (Eirene) [18, 19]. It is widely used in the fusion community and it was already applied to the simulation of liquid metal divertors [14, 20, 21]. Previous versions of the SOLPS package were also employed [22] for similar purposes.

The 2D multi-species description in B2.5 adopts classical parallel and anomalous perpendicular transport, with coefficients adjusted to match radial decay lengths from scaling laws or from experiments. Atomic databases such as ADAS [23] and AMJUEL [24] are included.

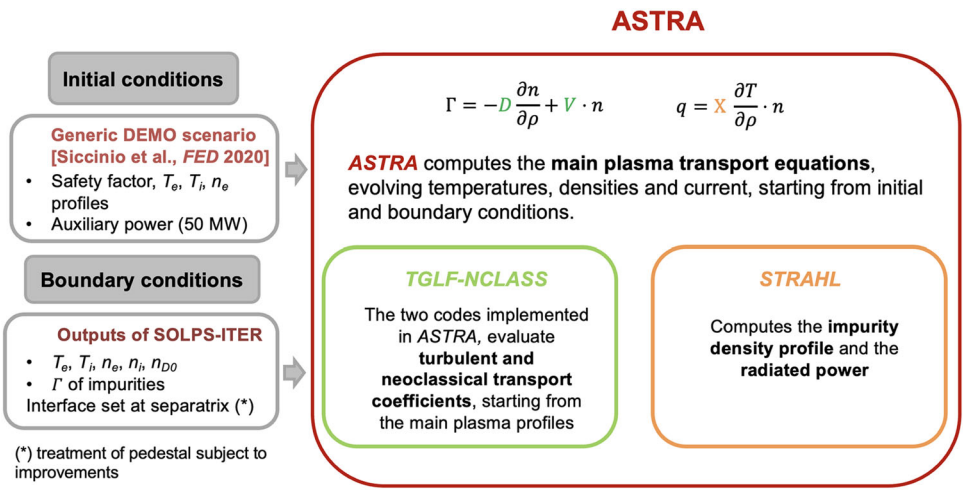

Fig. 1 Schematic representation of the ASTRA workflow. The auxiliary power was implemented as ECRH power

LM Target Model: FreeFem++

FreeFem++ [17] is an open-source programming framework for the solution of partial differential equations based on the finite-element method. It allows to efficiently solve the 2D heat conduction equation accounting for the actual divertor target material, shape and cooling strategy. In the specific case of an LMD, the CPS layer on top of the solid substrate, which includes the cooling channels, is treated in a simplified way, namely as a solid layer with averaged thermal properties evaluated by the law of mixtures, assuming pure Li/Sn.

Given the incoming plasma heat flux as computed by SOLPS-ITER and the characteristics of the active cooling system, which are taken into account by enforcing a Robin-type boundary condition, the outputs of the model are the temperature distribution in the divertor target - to be compared with material limits to assess their compatibility - and the metal evaporation flux for each poloidal location. This is summed to sputtering to determine the total impurity emission rate from the target, which is then fed back to SOLPS-ITER. The currently implemented coupling scheme represents a refinement of the one described in [25].

Core Plasma Model: ASTRA/STRAHL

ASTRA (Automated System for TRansport Analysis) is a flexible programming system capable of solving predictive or interpretive transport problems in the confined plasma [26]. The code computes the magnetic equilibrium and transport coefficients, and solves the transport equations for the main plasma parameters averaged over magnetic surfaces. In this way, the domain between the magnetic axis and the separatrix is treated as 1.5D.

The modular nature of ASTRA is employed to tailor the modelling strategy to the problem at hand. Specifically, a realistic description of the transport of impurities and the consequent radiation losses in the core plasma is achieved by coupling the STRAHL code [27] to ASTRA, as done in [28, 29]. Moreover, the turbulent and neoclassical transport coefficients are obtained by means of the TGLF and NCLASS routines, respectively. A schematic representation of the ASTRA workflow is provided in Fig. 1.

In the present work, separatrix-averaged values of electron temperature, impurity density and electron density as computed by SOLPS-ITER are used as boundary conditions for the ASTRA-STRAHL calculations.

Results for the SOL-Target Model

Applying the model to an LPD case allows to simplify the simulation setup and the comparison with experimental data in ITER-relevant heat and particle flux conditions, while keeping a low computational time. For this reason, as a first test bench, the coupled SOL plasma - target model was applied to simulate experiments performed in the Magnum-PSI [30] linear plasma device. The application of SOLPS-ITER to an LPD was only recently made possible [31, 32].

Two configurations were considered: a first one, with a solid (W) target, to check whether the computed temperatures are compatible with experimental measurements; and a second one with a CPS target filled with Li. The SOLPS-ITER calculation domain for Magnum-PSI is schematized in Fig. 2.

For all simulations, the target thermal behavior is computed based on the heat flux distribution over the top surface, as provided by SOLPS-ITER, and on the active cooling at the bottom, which is accounted for by adopting a

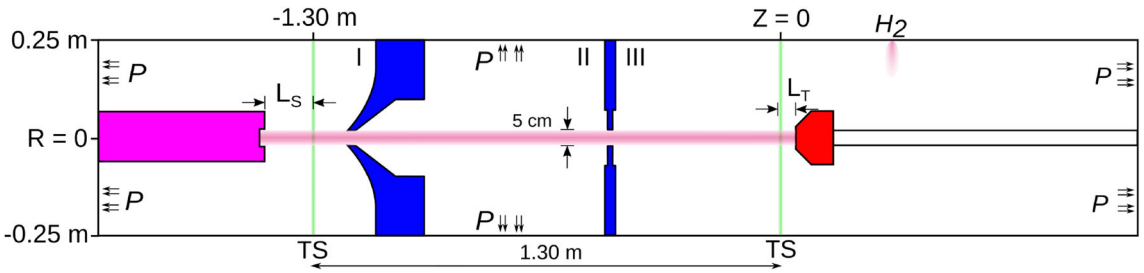

Fig. 2 Schematic of the Magnum-PSI calculation domain

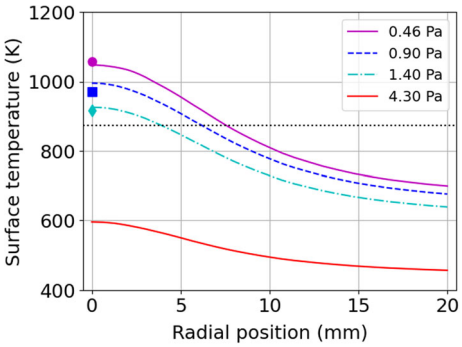

Fig. 3 Computed surface temperature (lines) and pyrometer measurements at target center (markers) for different neutral pressures in the target chamber. The black dotted line represents the lower measurement limit for the pyrometer

Robin-type boundary condition, enforcing the equality of the conduction heat flux in the target and of the convection heat flux to the coolant at each point of the bottom surface:

$$-k(T)\frac{\partial T}{\partial n} = h_{cool}(T - T_{water}) \tag{1}$$

On the left hand side of equation (1), k is the temperature dependent heat conductivity of the target material and $\frac{\partial T}{\partial n}$ is the normal derivative of the temperature field (T is the local surface temperature). h_{cool} is a global heat transfer coefficient computed as the inverse of the series of thermal resistances associated to conduction in the target holder and to convection with the coolant:

$$\left(\frac{1}{h_{water}} + \frac{\delta_{Cu}}{k_{cu}} + \frac{\delta_{iso}}{k_{iso}}\right)^{-1} \sim 3500\ \mathrm{W/m^2/K} \tag{2}$$

where $h_{water} = 4164\ \mathrm{W/m^2/K}$ is the convection heat transfer coefficient with the coolant, computed based on well known single phase heat transfer correlations for circular pipes [33] based on the cooling channel dimensions ($D_{channel} = 10$ mm) and on the coolant flow conditions ($T_{water} = 25\ ^\circ$C, $u_{water} = 2.9$ m/s), $\delta_{Cu} = 4$ mm is the thickness of the copper holder between the water and the target and $\delta_{iso} = 0.3$ mm is the thickness of the isolation foil (made of HiTherm HT1220, with thermal conductivity $k_{iso} = 10\ \mathrm{W/m/k}$) between copper and target.

Solid Target

For the solid W target, different simulations were performed, considering values of the neutral pressure in the target chamber ranging from 0.46 Pa to 4.30 Pa, the latter leading to a fully detached plasma condition. The simulation setup is essentially identical to the one in [32], with the difference that here the coupled target-SOL model is enabled. The results in terms of the computed radial distribution of the target surface temperature are reported in Fig. 3. As expected, as the gas pressure in the target chamber increases, the peak temperature is reduced following the lower target heat flux. Figure 3 also shows, depicted as markers, the pyrometer measurements at the target center for all the simulated cases except the higher pressure case (plotted as a dotted black line), for which the temperature at the target center fell below the measurement limit of the pyrometer. New experiments are planned in the future to extend the validation range of the coupling between SOLPS-ITER and the target model.

Figure 4 shows the temperature distribution inside the tungsten target for the lowest and highest pressure cases.

Li-Filled CPS Target

Recently, Magnum-PSI experiments were performed on liquid Li-filled CPS targets realized via 3D printing, an approach previously explored by Rindt et al. [34]. These experiments represent a further opportunity to achieve a preliminary validation of the SOL-target calculation framework. However, in this case comparing the simulation results with experimental data involves further difficulties with respect to the case of a solid W target. Indeed, the 3D printed CPS is characterized by a progressive reduction of the pore size moving towards the plasma-facing surface, a situation for which the previously adopted treatment, which relied on the law of mixtures with uniform porosity $\gamma = V_{Li}/(V_{Li} + V_{CPS})$, becomes questionable. Furthermore, liquid Li-filled CPSs are subject to changes in surface emissivity which make temperature measurements difficult [34].

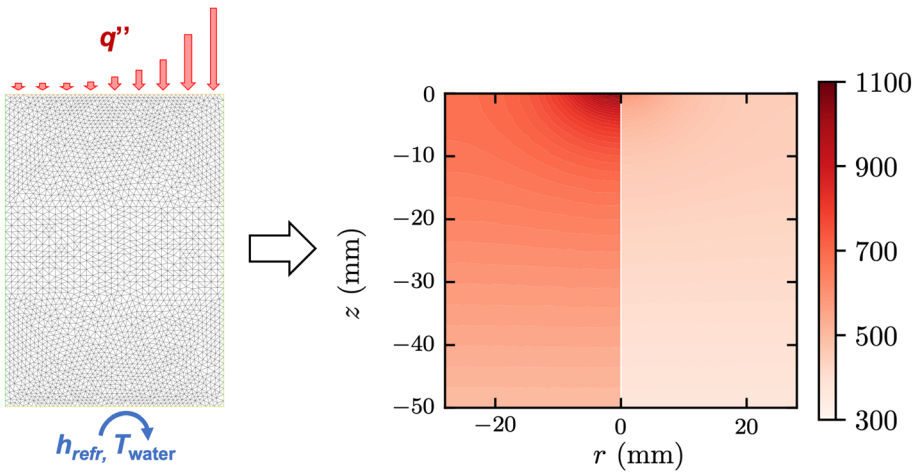

Fig. 4 FreeFem++ mesh of the Magnum-PSI target with boundary conditions schematically indicated (left) and target temperature distributions for the 0.46 Pa and the 4.30 Pa cases (right)

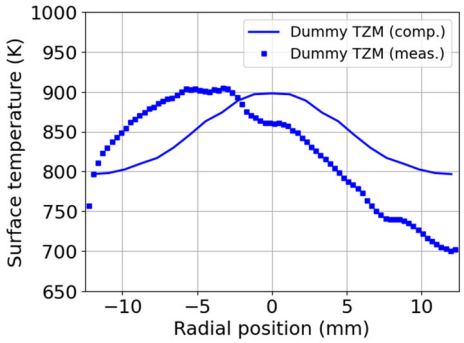

Fig. 5 Computed (solid line) and measured (square markers) surface temperature distribution for the dummy TZM target

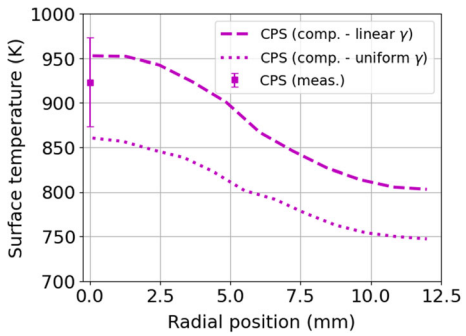

Fig. 6 Surface temperature distribution for the Li-filled CPS assuming a linear porosity (dashed line) and a uniform porosity (dotted line). The temperature measurement at the center of the target is also reported with a square marker, together with its uncertainty

To overcome this problem, a *dummy target* made in Titanium Zirconium Molybdenum alloy (TZM) and similar to the Li-filled CPS in terms of thermal properties, was employed before exposing the CPS itself. This allows to calibrate the thermal model in the simplest possible scenario, before exposing the porous targets, which are inherently more challenging in terms of experimental validation. The pressure during exposures is between 0.2 and 0.3 Pa as no additional gas puffing is introduced. Figure 5 reports simulation results for the TZM dummy target, together with the corresponding experimental data. The agreement is very good in terms of the peak target temperature, whereas the measured temperature distribution appears to be radially shifted by $\sim 2-5$ mm with respect to the target center, a feature which cannot be retrieved in the model (which assumes axial symmetry around the plasma axis, which corresponds to the center of the target) and which suggests that further assessment of the experimental data is needed. However, a detailed comparison is deemed to be beyond the scope of the present paper, which is rather concerned with the integrated modelling strategy and with preliminary results for what concerns the SOL-target coupling.

Moving to the actual Li-filled CPS target, two distinct simulations have been performed with different assumptions on the target porosity distribution, in view of the above-mentioned uncertainties. Specifically, a case with uniform porosity and one with linearly decreasing porosity (from 0.4 at the bottom to 0.0 at the top) have been considered. In both cases, as before, no additional gas puffing is considered. Results are shown in Fig. 6, and compared with the measured surface temperature at the target center. This preliminary comparison suggests that, as expected, reducing the CPS porosity towards the target surface allows to reproduce experimental results more closely. However, also this point requires further assessment. In more general terms, it can be stated that evaluating thermal properties of 3D printed or sintered W is crucial to correctly evaluate the surface temperature.

Ongoing Work on SOL-Core Coupling

The modelling effort here presented is ultimately aimed at the self-consistent simulation of the EU-DEMO plasma in the presence of a liquid metal divertor, considering an EU-DEMO configuration with a liquid Li or Sn divertor while keeping the same envelope as for the baseline (W) divertor.

As far as the SOL plasma is concerned, a first set of calculations for the EU-DEMO configuration with a liquid Li or Sn divertor was reported in [14]. In that work, the target-SOL coupling was in place, but a simplified fluid model for the neutrals was employed and the core plasma model was not included. Simulations including the new capabilities demonstrated in the foregoing section are ongoing.

As far as the core plasma is concerned, first ASTRA-STRAHL-TGLF simulations have been set up, considering a single source of impurities, respectively of Li and Sn, which is computed based on the available SOLPS-ITER calculations.

However, integrated modelling results are still preliminary and will be presented in a later communication. It is also worth mentioning that for turbulent transport, alongside with the currently adopted TGLF model, QuaLiKiz is also being considered [35, 36]. Similarly, for the neoclassical transport of heavy impurities, represented by Sn in the present application, it is planned to adopt the recently developed FACIT code [37].

Conclusions and Perspective

In this paper, a strategy for performing integrated plasma simulations for fusion devices using liquid metal targets was proposed. A subset of the proposed models, and specifically those pertaining to the SOL-target coupling, was applied to Magnum-PSI as a first test bench, showing promising results, although a more thorough validation of the erosion model against Magnum-PSI data is planned. SOL-core results are instead still preliminary and will be reported in a future communication.

Ongoing work regards the application of the integrated modelling framework to tokamaks for which experiments with liquid metal divertors were performed (COMPASS and AUG), thus allowing to preliminary validate both the SOL-target model and the core impurity transport model, so providing more confidence in applying to the EU DEMO.

Acknowledgements This work has been carried out within the framework of the EUROfusion Consortium, funded by the European Union via the Euratom Research and Training Programme (Grant Agreement No 101052200—EUROfusion). Views and opinions expressed are however those of the author(s) only and do not necessarily reflect those of the European Union or the European Commission. Neither the European Union nor the European Commission can be held responsible for them.

Author Contributions Conceptualisation: GFN, JG, CM, FS, EW, RZ; Data curation: GFN, JG, EB, TL; Formal Analysis: GFN, JG, EB, TL; Funding acquisition: FS, EW, RZ; Investigation: GFN, JG, EB, TL, Methodology: GFN, JG, EB, TL, Project administration: GFN, FS, EW, RZ, Software: GFN, JG, EB, TL; Writing—original draft: GFN, EB; Supervision: CM, FS, EW, RZ Visualisation: JG, EB; Writing—review and editing: all authors.

Funding Open access funding provided by Politecnico di Torino within the CRUI-CARE Agreement. The research leading to these results received funding from the European Union via the Euratom Research and Training Programme under Grant Agreement No 101052200.

Availability of Data and Materials The datasets generated during and/or analysed during the current study are available from the corresponding author on reasonable request.

Declarations

Conflict of interest The authors have no conflicts of interest to declare that are relevant to the content of this article.The authors declare no competing interests.

Ethical Approval Not applicable.

References

1. A.J.H. Donné, (ed.): European research roadmap to the realisation of fusion energy. EUROfusion, Boltzmannstrasse 2 85748 Garching / Munich, Germany (2018)
2. R.A. Pitts, S. Carpentier, F. Escourbiac, T. Hirai, V. Komarov, S. Lisgo, A.S. Kukushkin, A. Loarte, M. Merola, A. Sashala Naik, R. Mitteau, M. Sugihara, B. Bazylev, P.C. Stangeby, A full tungsten divertor for ITER: Physics issues and design status. J. Nucl. Mater. 438, 48–56 (2013). https://doi.org/10.1016/j.jnucmat.2013.01.008.Proceedings of the 20th International Conference on Plasma-Surface Interactions in Controlled Fusion Devices
3. ...R. Wenninger, R. Albanese, R. Ambrosino, F. Arbeiter, J. Aubert, C. Bachmann, L. Barbato, T. Barrett, M. Beckers, W. Biel, L. Boccaccini, D. Carralero, D. Coster, T. Eich, A. Fasoli, G. Federici, M. Firdaouss, J. Graves, J. Horacek, M. Kovari, S. Lanthaler, V. Loschiavo, C. Lowry, H. Lux, G. Maddaluno, F. Maviglia, R. Mitteau, R. Neu, D. Pfefferle, K. Schmid, M.

Siccinio, B. Sieglin, C. Silva, A. Snicker, F. Subba, J. Varje, H. Zohm, The DEMO wall load challenge. Nucl. Fus. **57**(4), 046002 (2017). https://doi.org/10.1088/1741-4326/aa4fb4
4. ...J.H. You, G. Mazzone, E. Visca, H. Greuner, M. Fursdon, Y. Addab, C. Bachmann, T. Barrett, U. Bonavolontà, B. Böswirth, F.M. Castrovinci, C. Carelli, D. Coccorese, R. Coppola, F. Crescenzi, G. Di Gironimo, P.A. Di Maio, G. Di Mambro, F. Domptail, D. Dongiovanni, G. Dose, D. Flammini, L. Forest, P. Frosi, F. Gallay, B.E. Ghidersa, C. Harrington, K. Hunger, V. Imbriani, M. Li, A. Lukenskas, A. Maffucci, N. Mantel, D. Marzullo, T. Minniti, A.V. Müller, S. Noce, M.T. Porfiri, A. Quartararo, M. Richou, S. Roccella, D. Terentyev, A. Tincani, E. Vallone, S. Ventre, R. Villari, F. Villone, C. Vorpahl, K. Zhang, Divertor of the European DEMO: engineering and technologies for power exhaust. Fus. Eng. Des. **175**, 113010 (2022). https://doi.org/10.1016/j.fusengdes.2022.113010
5. R. Kembleton, M. Siccinio, F. Maviglia, F. Militello, Benefits and challenges of advanced divertor configurations in DEMO. Fus. Eng. Des. **179**, 113120 (2022). https://doi.org/10.1016/j.fusengdes.2022.113120
6. S. Roccella, G. Dose, R. de Luca, M. Iafrati, A. Mancini, G. Mazzitelli, CPS based liquid metal divertor target for EU-DEMO. J. Fusion Energ. (2020). https://doi.org/10.1007/s10894-020-00263-4
7. P. Rindt, J.L. van den Eijnden, T.W. Morgan, N.J. Lopes Cardozo, Conceptual design of a liquid-metal divertor for the European DEMO. Fus. Eng. Des. **173**, 112812 (2021). https://doi.org/10.1016/j.fusengdes.2021.112812
8. R.E. Nygren, F.L. Tabares, Liquid surfaces for fusion plasma facing components-A critical review: Physics and PSI. Part I. Nucl. Mater. Energy **9**, 6–21 (2016). https://doi.org/10.1016/j.nme.2016.08.008
9. P. Rindt, T.W. Morgan, M.A. Jaworski, N.J. Lopes Cardozo, Power handling limit of liquid lithium divertor targets. Nucl. Fus. (2018). https://doi.org/10.1088/1741-4326/aad290
10. Mazzitelli, G., Apicella, M.L., Frigione, D., Maddaluno, G., Marinucci, M., Mazzotta, C., Ridolfini, V.P., Romanelli, M., Szepesi, G., Tudisco, O., Team, F., FTU results with a liquid lithium limiter. Nucl. Fus. **51**(7), 073006 (2011). https://doi.org/10.1088/0029-5515/51/7/073006
11. G. Mazzitelli, M.L. Apicella, M. Iafrati, G. Apruzzese, F. Bombarda, F. Crescenzi, L. Gabellieri, A. Mancini, M. Marinucci, A. Romano, the FTU Team: experiments on the Frascati Tokamak upgrade with a liquid tin limiter. Nucl. Fus. **59**(9), 096004 (2019). https://doi.org/10.1088/1741-4326/ab1d70
12. J. Horacek, J. Cecrdle, D. Tskhakaya, R. Dejarnac, J. Schwartz, M. Komm, J. Cavalier, J. Adamek, S. Lukes, V. Veselovsky, J. Varju, P. Barton, S. Entler, Y. Gasparyan, E. Gauthier, J. Gerardin, J. Hromadka, M. Hron, M. Iafrati, M. Imrisek, M. Jerab, K. Kovarik, G. Mazzitelli, D. Naydenkova, G.V. Oost, R. Panek, A. Prishvitsin, J. Seidl, D. Sestak, M. Tomes, Y. Vasina, A. Vertkov, P. Vondracek, V. Weinzettl, Predictive modelling of liquid metal divertor: from COMPASS tokamak towards Upgrade. Phys. Scrip. **96**(12), 124013 (2021). https://doi.org/10.1088/1402-4896/ac1dc9
13. T.W. Morgan, P. Rindt, G.G. van Eden, V. Kvon, M.A. Jaworksi, N.J.L. Cardozo, Liquid metals as a divertor plasma-facing material explored using the Pilot-PSI and Magnum-PSI linear devices. Plasma Phys.d Control. Fus. **60**(1), 014025 (2017). https://doi.org/10.1088/1361-6587/aa86cd
14. G.F. Nallo, G. Mazzitelli, M. Moscheni, F. Subba, R. Zanino, SOLPS-ITER simulations of a CPS-based liquid metal divertor for the EU DEMO: Li vs Sn. Nucl. Fus. **62**(3), 036008 (2022). https://doi.org/10.1088/1741-4326/ac4867
15. M. Poradziński, I. Ivanova-Stanik, G. Pełka, R. Zagórski, Integrated core-SOL-divertor modelling for DEMO with tin divertor. Fus. Eng. Des. 124, 248–251 (2017). https://doi.org/10.1016/j.fusengdes.2017.04.131.Proceedings of the 29th Symposium on Fusion Technology (SOFT-29) Prague, Czech Republic, September 5-9, 2016
16. R. Zagórski, I. Ivanova-Stanik, V. Pericoli Ridolfini, M. Poradziński, F. Crisanti, Preliminary integrated core-SOL-divertor modelling for DTT tokamak with liquid metal divertor targets. Fus. Eng. Des. 146, 1916–1920 (2019). https://doi.org/10.1016/j.fusengdes.2019.03.065.SI:SOFT-30
17. F. Hecht, New development in FreeFem++. J. Numer. Math. **20**(3–4), 251–265 (2012). https://doi.org/10.1515/jnum-2012-0013
18. S. Wiesen, D. Reiter, V. Kotov, M. Baelmans, W. Dekeyser, A.S. Kukushkin, S.W. Lisgo, R.A. Pitts, V. Rozhansky, G. Saibene, I. Veselova, S. Voskoboynikov, The new SOLPS-ITER code package. J. Nucl. Mater. **463**, 480–484 (2015). https://doi.org/10.1016/j.jnucmat.2014.10.012
19. D.V. Borodin, F. Schluck, S. Wiesen, D. Harting, P. Börner, S. Brezinsek, W. Dekeyser, S. Carli, M. Blommaert, W.V. Uytven, M. Baelmans, B. Mortier, G. Samaey, Y. Marandet, P. Genesio, H. Bufferand, E. Westerhof, J. Gonzalez, M. Groth, A. Holm, N. Horsten, H.J. Leggate, Fluid, kinetic and hybrid approaches for neutral and trace ion edge transport modelling in fusion devices. Nucl. Fus. **62**(8), 086051 (2022). https://doi.org/10.1088/1741-4326/ac3fe8
20. E.D. Emdee, R.J. Goldston, J.D. Lore, X. Zhang, Predictive modeling of a lithium vapor box divertor in NSTX-U using SOLPS-ITER. Nucl. Mater. Energy **27**, 101004 (2021). https://doi.org/10.1016/j.nme.2021.101004
21. J.D. Lore, M.S. Islam, C.E. Kessel, D. Curreli, R. Maingi, M. Rezazadeh, S. Smolentsev, Simulation of liquid lithium divertor geometry using SOLPS-ITER. IEEE Trans. Plasma Sci. **50**(11), 4199–4205 (2022). https://doi.org/10.1109/TPS.2022.3166402
22. E.D. Marenkov, A.S. Kukushkin, A.A. Pshenov, Modeling the vapor shielding of a liquid lithium divertor target using SOLPS. Nucl. Fus. 4.3 code **61**(3), 034001 (2021). https://doi.org/10.1088/1741-4326/abd642
23. H. Summers, M. O'Mullane, Atomic data and modelling for fusion: the ADAS project. In: AIP Conference Proceedings, vol. 1344, pp. 179–187 (2011). American Institute of Physics
24. D. Reiter et al, The data file AMJUEL: additional atomic and molecular data for EIRENE. Forschungszentrum Juelich GmbH **52425** (2000)
25. J. Gonzalez, G.F. Nallo, E. Westerhof Self-consistent simulation of Magnum-PSI target in SOLPS-ITER with a Finite Element wall model. In: 48th EPS Conference on Plasma Physics 2022, ECA Volume 46A Paper P4b.114 (2022). http://ocs.ciemat.es/EPS2022PAP/pdf/P4b.112.pdf
26. G.V. Pereverzev, P.N. Yushmanov ASTRA Automated System for TRansport Analysis, 147
27. R. Dux, Strahl User Guide (2006). https://pure.mpg.de/rest/items/item_2143869/component/file_2143868/content
28. O. Linder, E. Fable, F. Jenko, G. Papp, G. Pautasso, The ASDEX Upgrade team, the EUROfusion MST1 team: Self-consistent modeling of runaway electron generation in massive gas injection scenarios in ASDEX upgrade. Nucl. Fus. **60**(9), 096031 (2020). https://doi.org/10.1088/1741-4326/ab9dcf
29. L. Casali, E. Fable, R. Dux, F. Ryter, Modelling of nitrogen seeding experiments in the ASDEX upgrade tokamak. Phys. Plasmas **25**(3), 032506 (2018). https://doi.org/10.1063/1.5019913
30. G. De Temmerman, M.A. van den Berg, J. Scholten, A. Lof, H.J. van der Meiden, H.J.N. van Eck, T.W. Morgan, T.M. de Kruijf, P.A. Zeijlmans van Emmichoven, J.J. Zielinski High heat flux capabilities of the Magnum-PSI linear plasma device. Fus. Eng. Des. 88(6), 483–487 (2013). https://doi.org/10.1016/j.fusengdes.2013.05.047.Proceedings of the 27th Symposium On Fusion Technology (SOFT-27); Liège, Belgium, September 24-28, 2012

31. M. Sala, E. Tonello, A. Uccello, X. Bonnin, D. Ricci, D. Dellasega, G. Granucci, M. Passoni, Simulations of Argon plasmas in the linear plasma device GyM with the SOLPS-ITER code. Plasma Phys. Control. Fus. **62**(5), 055005 (2020). https://doi.org/10.1088/1361-6587/ab7c4f
32. J. Gonzalez, R. Chandra, H.J. de Blank, E. Westerhof, Coupled simulations with SOLPS-ITER and B2.5-Eunomia for detachment experiments in Magnum-PSI. Plasma Phys. Control. Fus. **65**(4), 045009 (2023). https://doi.org/10.1088/1361-6587/acbe61
33. S. Kakac, R.K. Shah, W. Aung, Handbook of single-phase convective heat transfer. Wiley (1987)
34. P. Rindt, S.Q. Korving, T.W. Morgan, N.J.L. Cardozo, Performance of liquid-lithium-filled 3D-printed tungsten divertor targets under deuterium loading with ELM-like pulses in Magnum-PSI. Nucl. Fus. **61**(6), 066026 (2021). https://doi.org/10.1088/1741-4326/abf854
35. C. Bourdelle, J. Citrin, B. Baiocchi, A. Casati, P. Cottier, X. Garbet, F. Imbeaux, J. Contributors, Core turbulent transport in tokamak plasmas: bridging theory and experiment with qualikiz. Plasma Phys. Control. Fus. **58**(1), 014036 (2015). https://doi.org/10.1088/0741-3335/58/1/014036
36. B. Liu, S.Y. Dai, X.D. Yang, V.S. Chan, R. Ding, H.M. Zhang, Y. Feng, D.Z. Wang, Evaluation of edge transport and core accumulation of tungsten for cfetr with emc3-eirene and strahl. Nucl. Fus. **62**(12), 126040 (2022). https://doi.org/10.1088/1741-4326/ac95aa
37. D. Fajardo, C. Angioni, F.J. Casson, A.R. Field, P. Maget, P. Manas, J. the ASDEX Upgrade Team, Contributors, Analytical model for the combined effects of rotation and collisionality on neoclassical impurity transport. Plasma Phys. Control. Fus. 65(3), 035021 (2023). https://doi.org/10.1088/1361-6587/acb0fc

Authors and Affiliations

Giuseppe Francesco Nallo[1] · Jorge Gonzalez[2] · Elisabetta Bray[1] · Teobaldo Luda di Cortemiglia[3] · Chiara Marchetto[4] · Fabio Subba[1] · Egbert Westerhof[2] · Roberto Zanino[1]

✉ Giuseppe Francesco Nallo
giuseppefrancesco.nallo@polito.it

Jorge Gonzalez
J.GonzalezMunos@differ.nl

Elisabetta Bray
s292538@studenti.polito.it

Teobaldo Luda di Cortemiglia
teobaldo.luda.di.cortemiglia@ipp.mpg.de

Chiara Marchetto
chiara.marchetto@isc.cnr.it

Fabio Subba
fabio.subba@polito.it

Egbert Westerhof
E.Westerhof@differ.nl

Roberto Zanino
roberto.zanino@polito.it

[1] NEMO Group, Dipartimento Energia, Politecnico di Torino, Corso Duca degli Abruzzi 24, 10129 Turin, Italy

[2] DIFFER-Dutch Institute for Fundamental Energy Research, De Zaale 20, 5612 AJ Eindhoven, The Netherlands

[3] Max Planck Institute for Plasma Physics, 85748 Garching, Germany

[4] ISC-CNR, Dipartimento Energia, Politecnico di Torino, Corso Duca degli Abruzzi 24, 10129 Turin, Italy